Int. J. Radiation Oncology Biol. Phys. Vol. 21, pp. 71–78
Printed in the U.S.A.

0360-3016/91 $3.00 + .00

● *Original Contribution*

DOSE-VOLUME HISTOGRAMS

R. E. DRZYMALA, PH.D.,[1] R. MOHAN, PH.D.,[2] L. BREWSTER, M.S.,[2] J. CHU, PH.D.,[3] M. GOITEIN, PH.D.,[4] W. HARMS, B.S.[1] AND M. URIE, PH.D.[4]

[1]Mallinckrodt Institute of Radiology, Washington University School of Medicine, St. Louis, MO 63110; [2]Memorial Sloan-Kettering Cancer Center, New York, NY 10021; [3]University of Pennsylvania School of Medicine and the Fox Chase Cancer Center, Philadelphia, PA 19111; and [4]Massachusetts General Hospital, Department of Radiation Medicine, Boston, MA 02114 and Harvard Medical School

A plot of a cumulative dose-volume frequency distribution, commonly known as a dose-volume histogram (DVH), graphically summarizes the simulated radiation distribution within a volume of interest of a patient which would result from a proposed radiation treatment plan. DVHs show promise as tools for comparing rival treatment plans for a specific patient by clearly presenting the uniformity of dose in the target volume and any hot spots in adjacent normal organs or tissues. However, because of the loss of positional information in the volume(s) under consideration, it should not be the sole criterion for plan evaluation. DVHs can also be used as input data to estimate tumor control probability (TCP) and normal tissue complication probability (NTCP). The sensitivity of TCP and NTCP calculations to small changes in the DVH shape points to the need for an accurate method for computing DVHs. We present a discussion of the methodology for generating and plotting the DVHs, some caveats, limitations on their use and the general experience of four hospitals using DVHs.

Dose-volume histograms, Radiation therapy, Computerized treatment planning.

INTRODUCTION

Three-dimensional treatment planning involves a large body of dose information made available by volume dose calculations. The sheer volume of information may make it difficult to interpret and assimilate the data displayed as isodoses on a number of transverse, sagittal, coronal or oblique planes, as three-dimensional isodose surfaces, or as other forms of three-dimensional displays. Condensing the three-dimensional dose distribution data into dose-volume histograms enables one to graphically summarize the radiation distribution throughout the target volume and the anatomical structures of interest. A histogram may be plotted according to the usual mathematical definition, as the accumulated volume of those elements receiving dose in a specified dose interval against a set of equispaced dose intervals. This is referred to as a differential dose-volume histogram. We have found it more useful, however, to plot the data as the volume receiving a dose greater than or equal to a given dose against that dose over the expected dose range. These plots are actually cumulative dose-volume frequency distributions; we shall hereafter refer to them simply as dose-volume histograms (DVHs). In most instances, the volume is specified as the percentage of the total volume of a structure receiving dose within each interval; however, it may be more appropriate to specify absolute volume in some cases.

DVHs may be valuable in the planning process to check if dose is at an adequate level and uniform throughout the target volume, or for revealing the presence and extent of hot spots in adjacent normal tissues. DVHs may be used as a preliminary step in evaluating a treatment plan, or as a screening tool to select the best or most acceptable plan(s) from a group of plans before more extensive information is examined in the form of 2-D or 3-D isodose displays. [They may also be used as a graphical way of comparing different treatment plans in a single plot, and to produce measures of tumor control probability (TCP) or normal tissue complication probability (NTCP) (10, 11), allowing quantitative scoring and evaluation of plans.]

The use of dose-volume histograms has been reported in the literature (1, 3, 4, 6, 8, 10–12, 15) for the pancreas and prostate, but details of methods for their calculation have not been described. Four hospitals have participated in an NCI-sponsored contract studying three-dimensional photon treatment planning, and we present here their DVH techniques and experiences.

Supported in part by NCI Contracts NO1 CM-47316, NO1 CM-47695, NO1 CM-47696, NO1 CM-47697.

Reprint requests to: R. E. Drzymala, Mallinckrodt Institute of Radiology, Washington University School of Medicine, 510 S. Kingshighway Blvd., St. Louis, MO 63110.

METHODS AND MATERIALS

Each of the four institutions involved in this study developed their histogram code independently. Most of the features implemented are shared by all institutions, with differences occurring primarily in the handling of boundary regions and resolution. DVHs are calculated as follows: first, the boundaries of pertinent anatomical structures of the patient must be defined and the dose must be computed for the volume of interest. The anatomy is then subdivided into a volume grid of appropriate resolution. To arrive at the total volume for a particular structure, one sums those volume elements (voxels) lying within the structure. The dose for each voxel can be determined concurrently with voxel-summing so that, ultimately, all contributing voxels are accumulated within the appropriate dose bin of the histogram for each structure. The bin values are then plotted.

Anatomical representation

The three-dimensional image, usually composed of a contiguous sequence of computed tomographic (CT) scans, provides the basic anatomical representation of the patient. One can think of this volume as being subdivided into a three-dimensional grid of cuboid volume elements which is equispaced in the X and Y directions but may not be equispaced in the Z direction. (In our convention, each CT slice lies at a constant Z and each element in the slice is referenced by the X and Y coordinates of a point at its center.) One may divide the volume into contiguous "slabs" formed by the CT slices. These form a natural set of planes since it is through the CT images that the structures of interest are defined. If the scans are considered to just fill the volume they span, then the thickness of the n'th slab is equal to the distance between the $(n-1)$th and the $(n+1)$th slices. (The first and last scans have a thickness equal to their spacing from their nearest neighbor.) The volume of a voxel, therefore, is the product of the X and Y grid spacings and the slab thickness.

Optimum grid spacing and size

Computing a dose-volume histogram involves three-dimensional anatomical volume and radiation dose matrices. The three-dimensional matrix used for volume calculations need not be coincident, however, with the three-dimensional dose matrix nor the three-dimensional matrix of CT voxels. Dose calculations tend to be slow; usually a relatively coarse matrix is employed, but the matrix required for accurate volume estimation may be of much finer resolution. The accuracy of volume calculation, therefore, should not be limited by the dose matrix resolution. One can estimate the dose to each voxel of appropriate resolution by tri-linear interpolation from the dose matrix to the center of the voxel, thereby avoiding the need for a dose matrix with resolution equal to the volume grid. Dose resolution can then depend solely upon dose gradients in the region. If the voxel lies within a structure but not within the dose matrix, i.e., outside the calculation window, the dose to that voxel is considered to be zero. This can be a problem if the planner does not cover the entire region of interest receiving significant dose with the dose calculation window.

Volume. Attempts were made to determine the volume resolution necessary to achieve an acceptable level of accuracy through analyzing DVHs for various structures and manipulating the voxel size (4). As would be expected, small structures appeared most sensitive to increases in voxel size. Experimental data indicate that, for a constant dose matrix of comparable resolution, little change is evident in the DVH for the spinal cord residing in a fairly homogeneous dose region for a Hodgkins treatment plan if the voxel dimensions are less than 0.25 that of the structure. Volume estimation was on the average within 5% of the true value, but theory predicts errors up to 16% for extreme cases at this resolution. This results primarily from the errors accumulated while detecting the location of irregular contour boundaries with a regular rectangular grid of voxels. Changes of structure position in the volume grid help, since accumulated errors in boundary estimation average out. Accuracy, however, depends also upon the minimum of the structure, where the presence of a long, narrow but important appendage may require a finer resolution. Since greater resolution means a smaller voxel size and increased computation time (particulary in large structures), one should, as one group did, dynamically adjust the voxel size to the dimensions of the structure independently in X, Y and Z. This may be accomplished through the use of quadtrees and/or octrees.

Quite often the CT scan series covers only a portion of the organ of interest, which, if unaccounted for, can be a problem when interpreting DVHs. One possible solution involves the use of a set of standard volumes against which a computed volume could be compared. If the computed volume is significantly smaller than the standard size for the organ, additional volume can be added to the zero dose bin. This assumes, of course, that the CT series covers the region getting any significant dose.

Dose. The selection of grid spacing for the three-dimensional dose matrices involves compromise. The finer the grid, the greater the accuracy of dose calculation in regions of high dose gradients. The disadvantages of fine grid spacing include increased computation times and the creation of large disk files. In general, one must specify two criteria: 1) the desired dose accuracy, and 2) the maximum acceptable distance between the estimated and actual isodose contours. A dose interpolation would be acceptable if either criterion were met. The most stringent situation clearly occurs in regions of rapidly varying dose, for example, at the beam margins. A calculation of the error in the dose estimate when interpolating within regular rectangular grid indicates (Niemierko and Goitein, private communciation) that the required grid size depends on the detailed shape of the beam profile. In both the steepest and

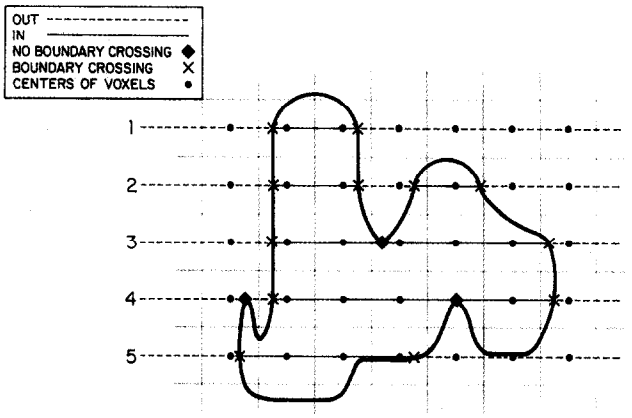

Fig. 1. Diagram showing scan lines (red) traversing an irregularly shaped contour (black) and a volume grid (blue) superposed. Each scan line demonstrates a different situation that the sampling algorithm must handle while searching for contour boundary crossings. Of particular importance are the conditions in lines 3, 4 and 5 where not all intersections of the scan line with the contour are boundary crossings.

most slowly varying regions, linear interpolation between grid points is a good approximation. It is in the intermediate regions, where the second gradient of the dose profile is large, that the greatest error is made. The best choice of grid spacing to achieve a given accuracy is dominated by the greatest allowable isodose position error, rather than the accuracy of dose estimation at a point. For most practical beams, in order to achieve an isodose positioning error of $\leq$ to delta—or a dose accuracy of $\leq$ to 2%, a grid spacing of about 2.5 times delta is needed. (Provided delta is $\geq$ 2 mm.) Thus 2% dose accuracy or 2 mm isodose positional accuracy (but not necessarily both) will be achieved with a grid spacing of 5 mm.

Assignment of voxels to a structure

Contours drawn on a contiguous parallel set of CT images usually define the structures. The cartesian volume matrix used to calculate the DVH is defined so that its Z-axis is normal to the sections on which the structure is defined. To determine which points of the volume matrix are within a structure, we consider one (X-Y plane) out of the volume matrix at a time and looping over each row equal to the y value at the center of the volume matrix voxels, find the intersections of the row with the contour(s) outlining the structure. If the X-Y planes of the volume matrix are not coincident with the CT slices, the outline(s) of the structure is obtained by interpolation between the closest CT sections on which the structure is defined. The algorithm selects and sorts only the transections (crossings of the boundary by the row) in the ascending order of distance from the beginning of the row. The voxels on the row whose centers lie between the odd numbered and the next even numbered transection are within the current structure while those whose centers follow the even numbered transections are outside the structure (see Fig. 1).

The volume of elements within a structure may accumulate in the appropriate dose interval bins "on the fly" as their location within a structure is ascertained. Alternatively, a three-dimensional matrix of tags identifying the structure (or segment of a multi-segment structure) of each volume element may be created prior to DVH calculations (12). The latter scheme is useful when combinations of structures are to be considered.

Binning

The range of expected dose values is divided into equispaced intervals in constructing a histogram. For each interval, the volumes of the voxels receiving dose within that interval are accumulated in the appropriate element of an array or bin. At the completion of the calculation, each bin in the array contains the summed volume of the voxels which received dose within the corresponding interval. Cumulative DVHs are obtained by adding volumes accumulated in each bin with the volumes in all bins corresponding to higher dose intervals, whereas to obtain differential DVHs, the volumes accumulated in the bins are not added.

For cumulative DVHs, an appropriate dose interval for the bins depends on the dose response curve for the structure of interest. It appears that 0.5 Gy ($\sim$ 1% of the prescription dose) is reasonable, whereas 2 Gy is crude. The group which used differential dose-volume histograms extensively concluded that, for this type of histogram, a crude bin interval of 2 to 5 Gy was advantageous in evaluating our breast plans.

Errors in calculating DVHs

The accuracy with which a DVH is estimated depends on the accuracy of estimating the boundaries of structures, the accuracy of dose calculations and interpolations of the dose matrix. Subjectivity and accuracy with which we outline structures on CT scans must all be considered. Where structure boundaries are not readily apparent, the process of structure outlining may be quite unreproducible. Contours are often entered into the computer with hard-to-control input devices, such as a mouse, joystick, trackball or digitizer pad, which introduces additional error. Improvements, including computer automation in some situations, are needed.

Since structures of interest can be quite irregularly shaped, the algorithm used to detect transections of the scan line with the structure contours is crucial. Not all intersections are transections. For example, invaginations and evaginations of the contour that touch the scan line then reverse direction should not be considered transections (Fig. 1, line 3). Also regions where the contour and scan line proceed superimposed (Fig. 1, line 5) are not transections except at one point where the contour traverses the scan line. Although the latter might seem like a rare special case, it does occur because of the discreet representation of structures on a pixel-based image.

A direct way to verify the DVH computation code before implementation is to create a few test phantoms of

known dimensions and dose assignments. A set of nested, concentric cubes was useful as a phantom; each rind formed therein had a different uniform dose. With the sides of the cubes oriented in parallel or perpendicularly to the scan line, this phantom provides a rigorous test for registration of the dose and volume matrices with the structure contours. This is particularly true if the inner cubes are excluded from the outer during the DVH calculation. Another appropriate test phantom is a cube with a rectangular notch cut in at one side. It is sensitive to boundary detection and the algorithm's ability to discriminate transections from intersections if a scan line is forced to coincide with the bottom edge of the notch. To complete the test, a cylindrical test phantom is helpful to assure the accuracy of the calculation for noncuboid shapes.

Addition and subtraction of DVHs

In some cases, volumes which are defined by some combination of more than one defined structure are of interest. For example, a DVH combining both right and left lungs may be desirable. In the case of overlapping structures, flexibility in structure definition is helpful. For instance, contours defining a patient's rectum and those defining a rectal tumor may overlap at some CT levels. One might want a histogram of all those points within the rectum, or only those points within the rectum but outside the tumor volume. On the other hand, a union of both structures may be of interest. Similar situations can occur when one structure is completely contained within another.

Separation and combination of structures could occur at the time of drawing their contours on CT images, but often this is not a practical nor the most flexible approach. One method of specifying and computing DVHs of such combinations of structure is by using a system of logical operators, such as 'and,' 'or,' 'not,' 'inside,' and 'outside.' Using the example of rectal cancer, the points within the rectum but not within the target would be specified as 'inside rectum and outside target.' The sum of both structures would be 'inside rectum or inside target.' The process of DVH calculation then becomes a matter of determining, for each point of the volume grid, whether the point lies within the logically specified region.

One method has been developed which allows the isolation of individual structures, as well as addition and subtraction operations on structures. It involves the construction of a user-specified hierarchy among anatomical structures prior to histogram calculation. The hierarchy level assigned to each structure is used to determine in which structure a given dose matrix point is considered to rest. This is necessary when structures overlap at the point.

The user assigns a hierarchy number to each anatomical structure of interest, with a higher number corresponding to a higher priority. This is done interactively for each series of histograms desired. To assign each grid point in the three-dimensional dose matrix to the structure containing the point, a corresponding matrix of structures, "tag," is created (12). Each element of the tag matrix has the same position in space as the corresponding element in the dose matrix, and is given a value related to an anatomical structure and its segment number. Since the tag matrix points are assigned values in ascending order of hierarchy, points common to more than one region will be set to the tag value corresponding to the structure with the highest hierarchy. This procedure results in a 3-D matrix of tags associating a structure with each dose point, thereby telling us in which structure any given dose matrix point is considered to rest.

With ambiguities thus resolved, the addition of two disjointed structures is accomplished by simply adding the corresponding dose level bins for the two structures, while the addition and subtraction of overlapping structures is done by proper assignment of hierarchies, and is carried out in the production of the structure tag matrix. For example, a structure contained within another can be subtracted out by assigning the inner structure a higher priority.

RESULTS

Comparisons among the institutions

Three of the four institutions participated in a comparison of the different calculation methods for producing cumulative DVHs. Each participant used the same concentric cube phantom containing contours and doses as described above. The resulting plots were essentially the same ($\pm$ 1 bin), with differences being attributable to the different resolutions employed and the way in which each program handled the boundaries of structure contours. It is difficult to assess the importance of the differences to clinical evaluation of the plans. We have observed, however, that small differences between histograms can affect TCP and NTCP calculations significantly (see also Discussion and Conclusion).

Examples of cumulative dose-volume frequency distributions

Figures 2 through 5 are examples of cumulative dose-volume histograms. We should mention some useful aspects of the graphic presentation. We have found it convenient to include both absolute dose and volume along with normalized relative values on the same plot. This can be easily accomplished by labeling four sides of the plot. An overlaid grid (not shown) helps to make the inspection of the curves more quantitative. When comparing different treatment plans, it is advantageous and, indeed, necessary to superimpose the DVH curves, labeled and appropriately color coded and/or patterned, on the same plot (Fig. 5). Differences are much more obvious when overlaid on the same plot. It is no accident that the one group which did not do this found DVHs less helpful in their assessment than did the other three groups.

Figure 2 is an example of a DVH computed for a target

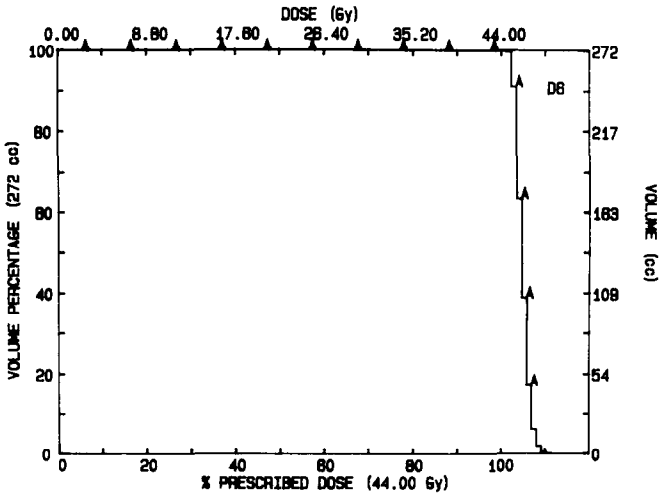

Fig. 2. An example of a cumulative dose-volume frequency distribution or histogram (DVH) computed and plotted for a structure that has a uniformly high dose throughout its volume. Typically, the volume is summed with that in intervals of higher dose and plotted against the dose intervals. The volume and dose may be absolute or normalized values, normalized to total volume or prescribed dose, respectively.

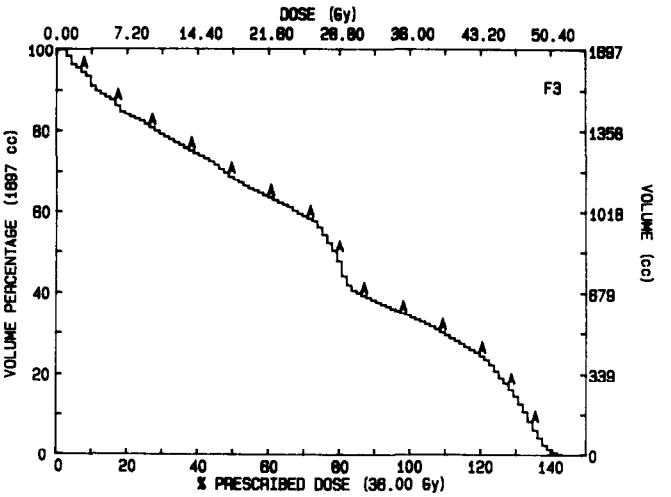

Fig. 3. The DVH depicted in this figure represents a structure having a dose distribution that is heterogeneous over the dose range. This is exemplified by a slope of approximately 45 degrees over much of the dose range. The plot makes no statement about the location of the dose. It could result from the structure residing in a dose gradient region or a dotted distribution of variable dose. (This is, however, a rather unlikely occurrence for teletherapy photon beams.)

volume which has a high, fairly uniform dose. The DVH under such circumstances approximates a step-function. Large, steep drops in the DVH ordinate are indicative of a large percentage of the volume having a similar dose. A plan giving this shape DVH for the target volume with the step at or just above the prescription dose would be close to ideal. This is contrasted with the curve of Figure 3 where we have a relatively shallow and constant slope. This curve represents a heterogeneous dose distribution in the volume of interest. The concave curve in Figure 4 represents a structure, the majority of which receives a low dose, but with one or more small hot spot(s). Not shown is the trivial case where the structure receives little or no dose. This case would appear as a step from 0 to 100% in the left-most bin and verifies that the structure is far removed from the radiation beams and their scattered radiation.

Differential dose-volume histograms (not shown) are true histograms. These plot the absolute or relative volume in each dose interval directly which can facilitate comparisons between dose bins of a histogram. True histograms also have a finer structure, possibly offering more detail for analysis. When multiple histograms from different plans are overlaid, the appearance of differential histograms is confusing. This is less of a problem with cumulative histograms. Plotting the cumulative dose-volume histogram as a "smoothed" line graph in contrast to its choppy appearance in the figures would serve to distinguish it further from the plots of true histograms. One approach would be to connect the right-most corners of adjacent bins with a straight line. One should remember that the plots should reflect the units of volume per dose interval, not discreet dose values. Using a nonlinear volume axis when plotting cumulative dose-volume histograms may help to observe fine structure in some regions of the curves (see Fig. 6).

Limitations of dose-volume histograms and some alternatives

DVHs graphically summarize dose distribution within an anatomic structure. While they provide information on the existence and magnitudes of hot and cold spots, they indicate neither where, within a structure, a hot spot

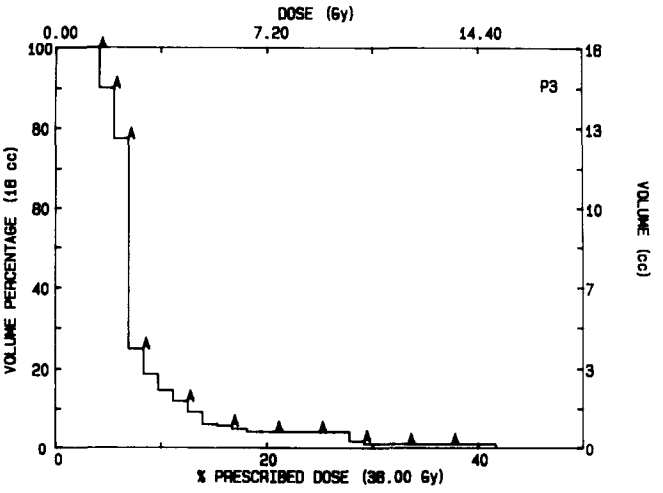

Fig. 4. The concave appearance of this DVH is indicative of a structure receiving predominantly low dose, but with one or more relatively small, higher dose regions.

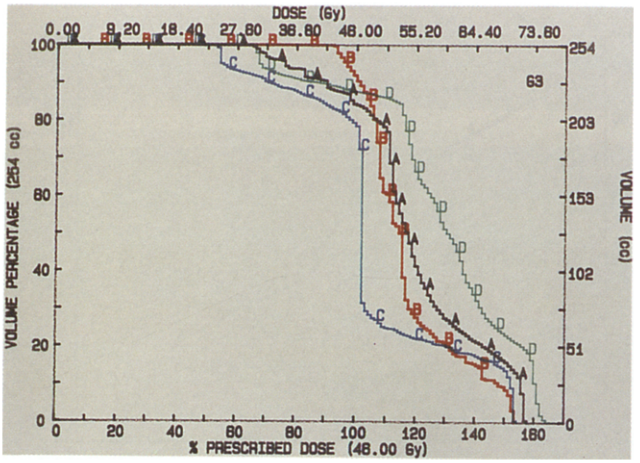

Fig. 5. Superimposed DVHs for the bladder comparing different treatment plans for cancer of the prostate. Color coding and repetitive labeling distinguish the curves.

occurred, nor whether a hot spot occurred in one or several disconnected regions. This may be more of a problem for some organs than others. The location of hot and cold spots in a structure may be dissected with other approaches.

In the spinal cord, for instance, a hot spot which transects the cord could have very different implications than one which was purely superficial. A solution to this problem might be a plot of the radial extent of the dose above a critical threshold as a function of length along the cord (again with a reduction in dimensionality).

The Dose Area Frequency Distribution (or Dose Area Histogram) is appropriate for skin and other anatomic surfaces, such as the rectum and bladder. DAHs are similar to DVHs, but with a reduction in dimensionality. They could be used in the planning process to predict and evaluate skin reactions for various types of treatments. In this case, the histogram would accumulate the surface areas of elements of the skin in the area of treatment as a function of the dose they received. As with volumes, contours can be used to define the surface of interest. The dimensions of each surface element are obtained from the spacing along the contour and between contours (i.e., the gaps between CT slices), with the curvature of the body, along the contour line as well as perpendicular to it, necessarily taken into account. The accurate estimation of dose at points on the sloping skin surface (such as in tangential breast treatments) is a complex process.

Dose-length histograms may be of value for long, linear structures such as the optic nerves or their blood vessels.

Another limitation of DVHs is that, as with dose distributions, interpretation of the plot is rather subjective and the implications of small differences between DVHs are poorly understood at present. This would point to the value of an objective numeric score, such as tumor control probability or normal tissue complication probability, to provide objective rank when comparing plans. Furthermore, we have found that small changes in the DVHs at times resulted in significant differences in the computed TCP and NTCP values.

DVHs do not reflect the complexity of the field arrange-

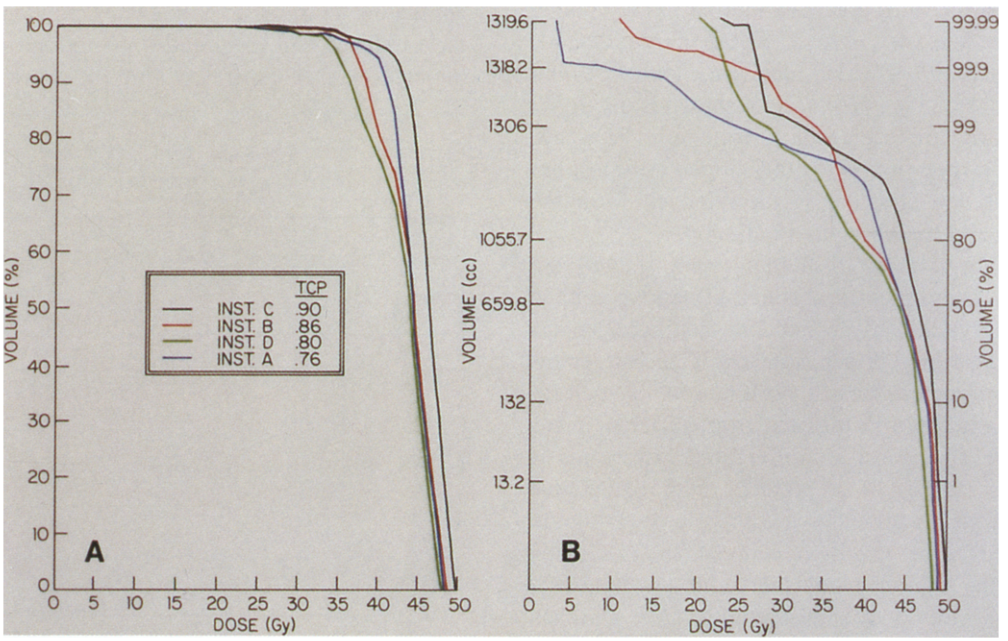

Fig. 6. In panel A are typical cumulative dose-volume histograms as normally plotted and superposed for use in this study. The inset gives the corresponding TCP calculations for the curves. Inspection of the curves as plotted does not reveal a good correlation of the curve positions with these numbers (see text). Replotting the volume axis with an expanded (panel B) scale shows a correlation with the small percentage of volume elements in the lower dose ranges.

ments, and, unlike dose distribution, this complexity cannot be inferred from the DVHs.

DISCUSSION AND CONCLUSION

The value of Cumulative Dose-Volume Frequency Distributions, less precisely termed Dose-Volume Histograms, has been investigated at four institutions participating in an NCI-sponsored contract exploring three-dimensional photon treatment planning. The usefulness of DVHs has been evaluated for eight anatomic sites. The specific findings for these and other sites are described elsewhere (1, 2, 3, 5, 7–9, 13–17). In our opinion, DVHs are a valuable means of summarizing, in graphic form, the large body of dose distribution information provided in 3-D planning. Their greatest strength is their ability to provide rapid screening of plans.

The detailed implementation of DVH computations could affect the shape of the plots significantly and accurate calculations are necessary if DVHs are to be widely used in the radiation therapy community. This would impact on estimates of TCP and NTCP as well, since the DVHs provide input data for these calculations and small differences in the DVHs have been observed in some circumstances to result in significant changes in computed TCP and NTCP values. For example, comparing TCP calculations with dose-volume histograms plotted in Figure 6, it is demonstrated that doses in a very small percentage of the total volume can have a significant impact in "ranking" treatment plans by TCP values. Inspecting the dose-volume histograms (panel A) as typically plotted, one would expect that the plans should be ranked C > A > B > D. Accordingly, more of the tumor volume would receive higher doses. The TCP calculation gives the order C > B > D > A. Replotting the same data with an expanded scale for the ordinate in panel B emphasizes volumes with higher and lower doses relative to those in the middle, and demonstrates a better correlation of the curves in the lower dose region with the calculated TCPs. The significance of this is not understood; however, it indicates that we should use methods that reduce the histogram to a single number cautiously.

The lack of information regarding the spatiality of dose distribution is one major limitation of DVHs; two- and three-dimensional dose displays are required for such analysis. This fact signifies that *DVHs cannot be the sole criterion for evaluating a plan, or disclosing the best treatment plan.* Complexity of field arrangement and reproducibility of patient set up are other important factors not taken into account by DVHs. However, these factors being equal, DVHs can be used effectively to evaluate and compare rival treatment plans.

REFERENCES

1. Austin-Seymour, M. M.; Chen, G. T. Y.; Castro, J. R.; Saunders, W. M.; Pitluck, S.; Woodruff, K. H.; Kessler, M. Dose volume histogram analysis of liver radiation tolerance. Int. J. Radiat. Oncol. Biol. Phys. 12:31–35; 1986.
2. Brown, A. P.; Urie, M. M.; Barest, G.; Cheng, E.; Coia, L.; Emami, B. N.; Galvin, J.; Kutcher, J.; Manolis, J.; Wong, J. W.; Yahalom, J. Three-dimensional treatment planning for Hodgkin's disease. Int. J. Radiat. Oncol. Biol. Phys. 21: 205–215; 1991.
3. Chen, G. T. Y.; Austin-Seymour, M.; Castro, J. R.; Collier, J. M.; Lyman, J. T.; Pitluck, S.; Saunders, W. M.; Zink, S. R. Dose volume histograms in treatment planning evaluation of carcinoma of the pancreas. In: Proceedings, Eight International Conference on Uses of Computers in Radiation Therapy, IEEE, ISBN 0-8186-0559-6; 1984:264–268.
4. Chu, J. C. H.; Richter, M. P.; Sontag, M. R.; Larsen, R. D.; Fong, K.; Bloch, P. Practice of 3-dimensional treatment planning at the Fox Chase Cancer Center, University of Pennsylvania. Radiother. Oncol. 8:137–143; 1987.
5. Coia, L. R.; Galvin, J.; Sontag, M.; Blitzer, P.; Brenner, H.; Cheng, E.; Doppke, K.; Harms, W.; Hunt, M.; Mohan, R.; Munzenrider, J.; Simpson, J. Three-dimensional photon treatment planning in carcinoma of the larynx. Int. J. Radiat. Oncol. Biol. Phys. 21:183–192; 1991.
6. Drzymala, R. E.; Harms, W. B.; Purdy, J. A. Dose-volume histograms for 3-D radiation treatment plans. Med. Phys. 14(3):460; 1987 (abstr.).
7. Emami, B.; Purdy, J. A.; Manolis, J.; Barest, G.; Cheng, E.; Coia, L.; Doppke, K.; Galvin, J.; LoSasso, T.; Matthews, J.; Munzenrider, J.; Shank, B. Three-dimensional treatment planning for lung cancer. Int. J. Radiat. Oncol. Biol. Phys. 21:217–227; 1991.
8. Goitein, M.; Miller, T. Planning proton therapy of the eye. Med. Phys. 10:275–283; 1983.
9. Kutcher, G. J.; Fuks, Z.; Brenner, H.; Brown, A. P.; Burman, C.; Cheng, E.; Coia, L.; Krippner, K.; Manolis, J. M.; Mohan, R.; Simpson, J. R.; Urie, M.; Vikram, B.; Wallace, R. Three-dimensional photon treatment planning for carcinoma of the nasopharynx. Int. J. Radiat. Oncol. Biol. Phys. 21:164–182; 1991.
10. Lyman, J. T. Complication probability as assessed from dose-volume histograms. Radiat. Res. 104:s-13–s-19; 1985.
11. Lyman, J. T.; Wolbarst, A. B. Optimization of radiation therapy, III: A method of assessive complication probabilities from dose-volume histograms. Int. J. Radiat. Oncol. Biol. Phys. 13:103–109; 1987.
12. Mohan, R.; Brewster, L. J.; Barest, G. D. A technique for computing dose volume histograms for structure combinations. Med. Phys. 14(6):1048–1052; 1987.
13. Munzenrider, J. E.; Doppke, K. P.; Brown, A. P.; Burman, C.; Cheng, E.; Chu, J.; Chui, C.; Drzymala, R. E.; Goitein, M.; Manolis, J. M.; Nori, D.; Simpson, J. R.; Solin, L.; Urie, M. M. Three-dimensional treatment planning for paraaortic node irradiation in patients with cervical cancer. Int. J. Radiat. Oncol. Biol. Phys. 21:229–242; 1991.
14. Shank, B.; LoSasso, T.; Brewster, L.; Burman, C.; Cheng, E.; Chu, J. C. H.; Drzymala, R. E.; Manolis, J.; Pilepich, M. V.; Solin, L. J.; Tepper, J. E.; Urie, M. M. Three-dimensional treatment planning for post-operative treatment of rectal carcinoma. Int. J. Radiat. Oncol. Biol. Phys. 21:253–265; 1991.
15. Shipley, W. U.; Tepper, J. E.; Prout, G. R.; Verhey, L. J.; Mendiondo, O. A.; Goitein, M.; Koehler, A. M.; Suite, H. D. Proton radiation as boost therapy for localized prostatic

carcinoma. JAMA 241:1912–1915; 1979.
16. Simpson, J. R.; Purdy, J. A.; Manolis, J. M.; Pilepich, M. V.; Burman, C.; Forman, J.; Fuks, Z.; Cheng, E.; Chu, J.; Matthews, J.; Mohan, R.; Solin, L.; Tepper, J.; Urie, M. Three-dimensional treatment planning considerations for prostate cancer. Int. J. Radiat. Oncol. Biol. Phys. 21:243:–252; 1991.
17. Solin, L. J.; Chu, J. C. H.; Sontag, M. R.; Brewster, L.; Cheng, E.; Doppke, K.; Drzymala, R. E.; Hunt, R. E.; Kuske, R.; Manolis, J. M.; McCormick, B.; Munzenrider, J. E. Three-dimensional treatment planning of the intact breast. Int. J. Radiat. Oncol. Biol. Phys. 21:193–203; 1991.